

Supporting Information for

Exfoliation of 2D van der Waals crystals in ultrahigh vacuum for interface engineering

Zhenyu Sun^{1,4}, Xu Han^{1,2}, Zhihao Cai^{1,4}, Shaosheng Yue^{1,4}, Daiyu Geng^{1,4}, Dongke Rong^{1,3}, Lin Zhao^{1,4}, Yi-Qi Zhang^{1,4}, Peng Cheng^{1,4}, Lan Chen^{1,4,5}, Xingjiang Zhou^{1,4}, Yuan Huang^{2*}, Kehui Wu^{1,4,5,6*}, and Baojie Feng^{1,4,6*}

¹Institute of Physics, Chinese Academy of Sciences, Beijing 100190, China

²Advanced Research Institute of Multidisciplinary Science, Beijing Institute of Technology, Beijing 100081, China

³School of Science, China University of Geosciences, Beijing 100083, China

⁴School of Physical Sciences, University of Chinese Academy of Sciences, Beijing 100049, China

⁵Songshan Lake Materials Laboratory, Dongguan, Guangdong 523808, China

⁶Interdisciplinary Institute of Light-Element Quantum Materials and Research Center for Light-Element Advanced Materials, Peking University, Beijing, 100871, China

*Corresponding authors: yhuang@bit.edu.cn, khwu@iphy.ac.cn, bjfeng@iphy.ac.cn

Figure S1 to S15

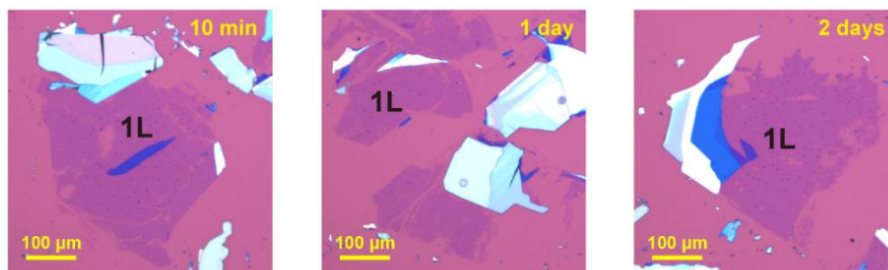


Figure S1. UHV exfoliation of monolayer MoS₂ on Au films. The exfoliation was performed after 10 min, 1 day, and 2 days, respectively, after the growth of Au films.

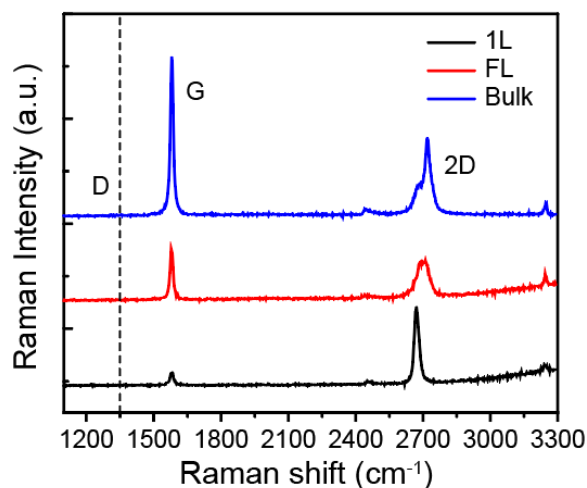


Figure S2. Raman spectra of the UHV-exfoliated graphene on MgO(100). 1L graphene shows a single-symmetric 2D peak ($\sim 2670 \text{ cm}^{-1}$) which is more intense than the G peak. The absence of the D peak at 1350 cm^{-1} indicates a negligible number of defects. For 1L and FL graphene, the increasing background above 2800 cm^{-1} originates from the MgO substrate.

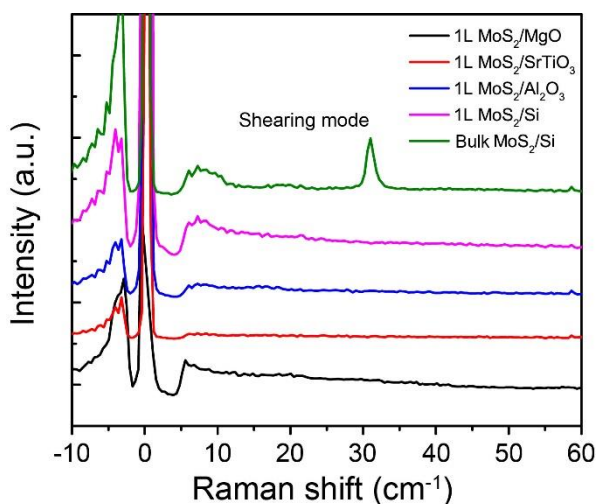


Figure S3. Ultra-low frequency Raman spectra for the UHV-exfoliated MoS₂ flakes on different single crystalline substrates. Monolayer MoS₂ is evidenced by the absence of the interlayer shearing mode, which is present on thicker samples.

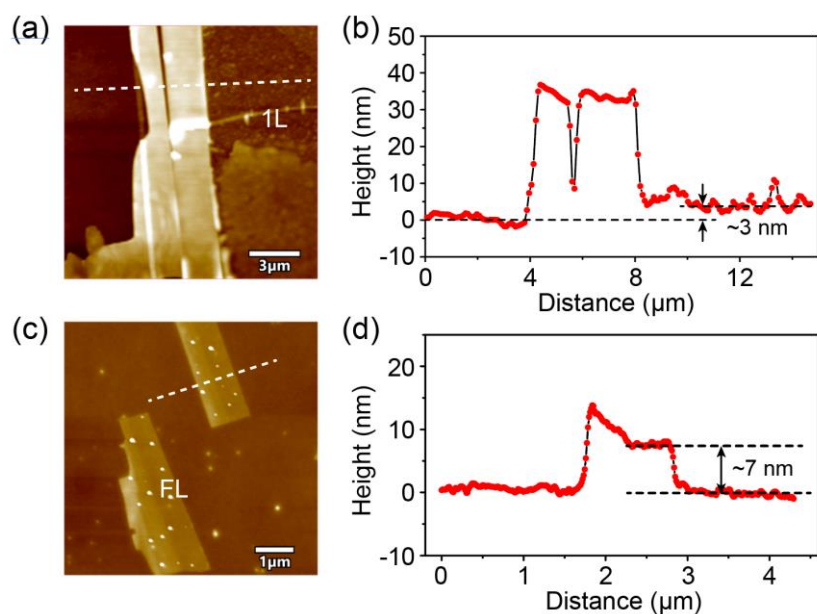


Figure S4. AFM characterization of the UHV-exfoliated Bi-2212/Si(111) and FeSe/SrTiO₃(100). (a,c) AFM images of monolayer Bi-2212/Si(111) and FeSe/SrTiO₃(100), respectively. (b,d) Line profiles along the white dashed lines in (a) and (c), respectively. Monolayer Bi-2212 is evidenced by the step height (≈ 3 nm), as shown in (b). The exfoliated FL FeSe nanoribbon thickness is about 7-10nm, as shown in (d).

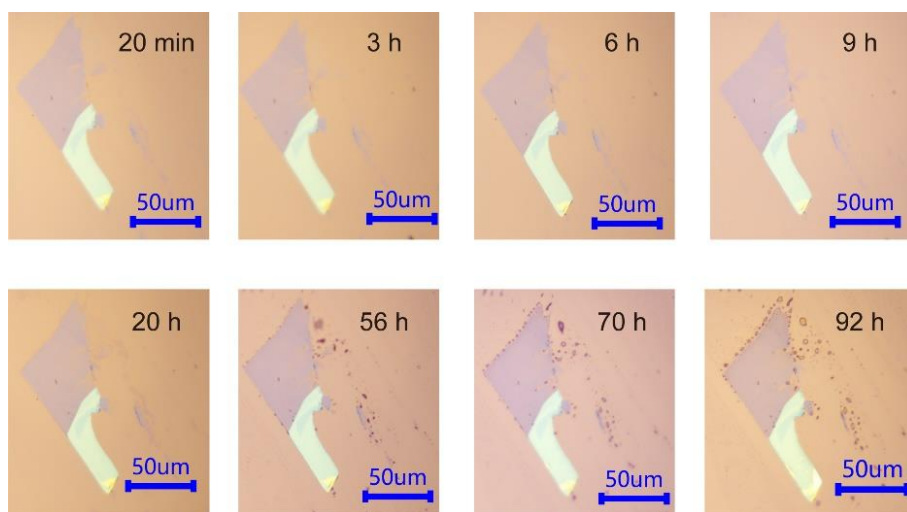


Figure S5. Optical images of the UHV-exfoliated FL black phosphorus (BP) on Au films exposed in air for different times. The surface exhibits a clear degradation after 56h in air.

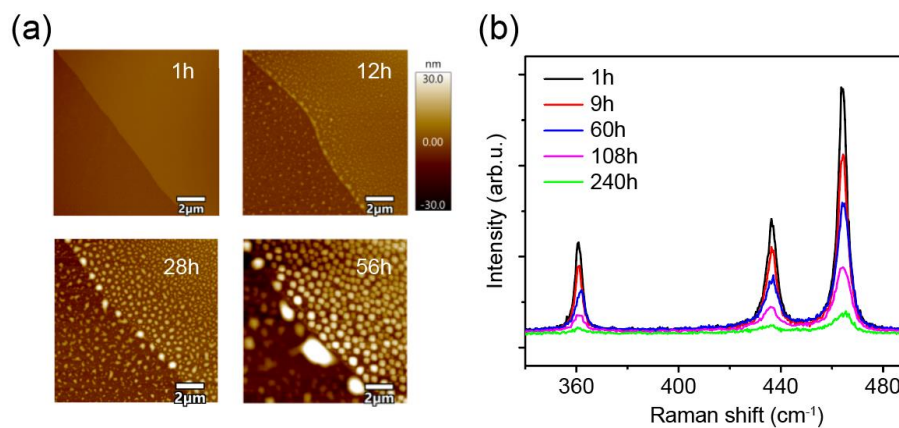


Figure S6. AFM images (a) and Raman spectra (b) of the UHV-exfoliated FL black phosphorus on Au films exposed in air for different times. The emergence of clusters and disappearance of Raman signal indicates a quick degradation of FL BP.

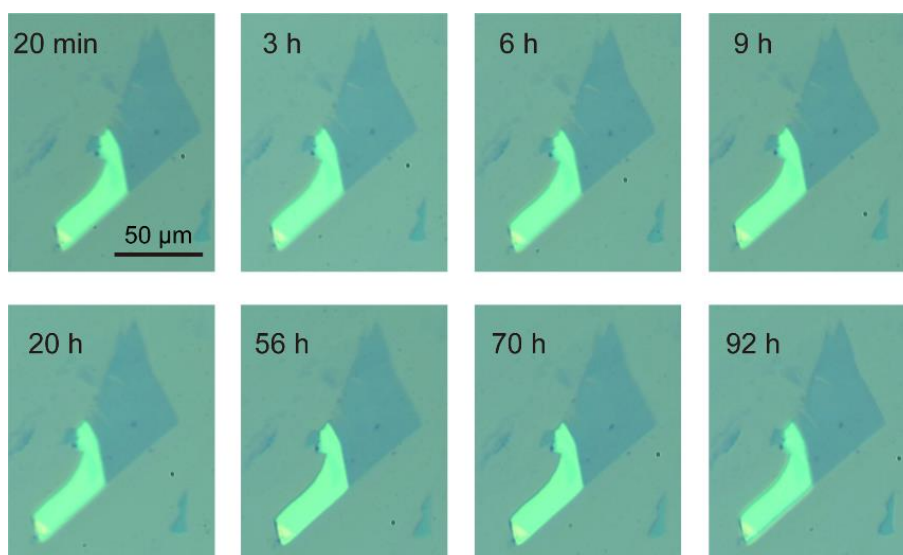


Figure S7. Optical images of the UHV-exfoliated FL BP in UHV for different times. The surface exhibits no visible degradation.

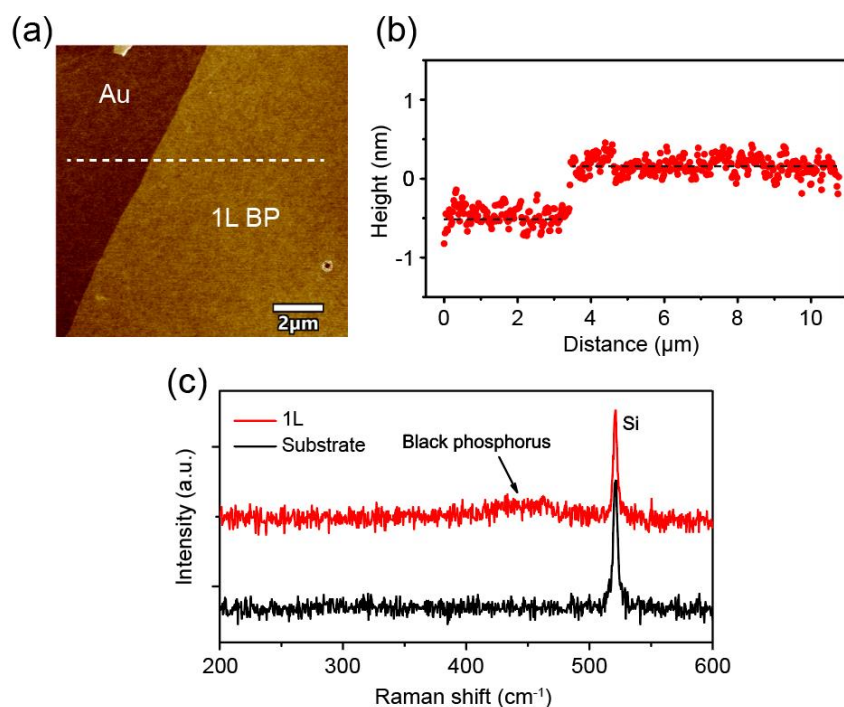


Figure S8. AFM and Raman characterization of the UHV-exfoliated millimeter-sized monolayer BP. (a) AFM image containing monolayer BP and the Au substrate. (b) Line profile along the white dashed line in (a). (c) Raman spectra acquired on the Au substrate and monolayer BP. The weak Raman signal at 420-480 cm⁻¹ originates from BP, which is absent on the substrate.

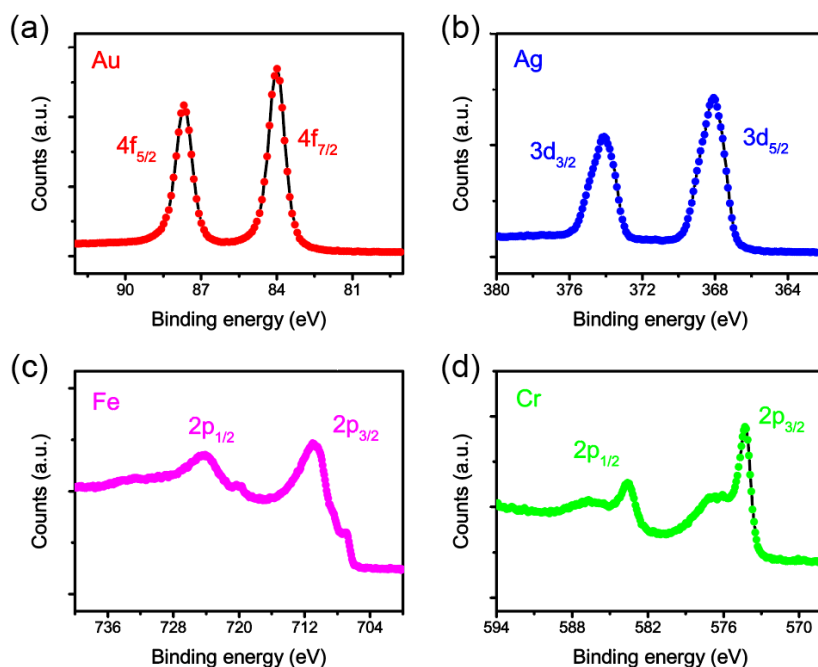


Figure S9. XPS characterization of the Au, Ag, Fe, and Cr films grown on SiO₂/Si, respectively. The characteristic peaks of each element are indicated.

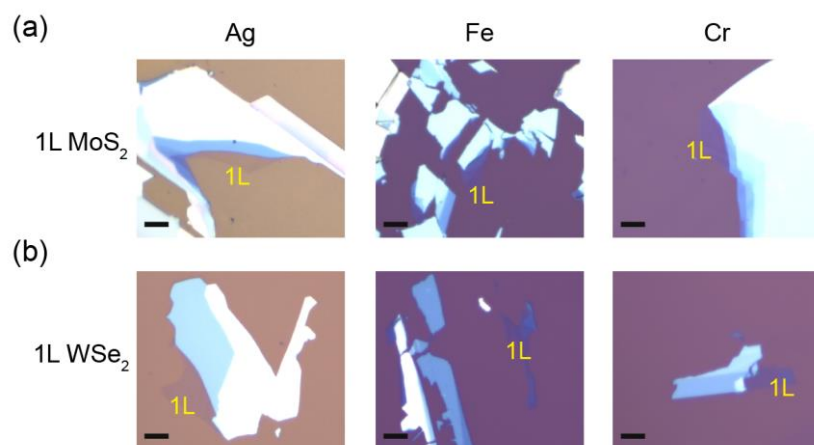


Figure S10. Optical images of the UHV-exfoliated monolayer MoS₂ (a) and WSe₂ (b) on Ag, Fe, and Cr films, respectively. Scale bar: 5 μ m.

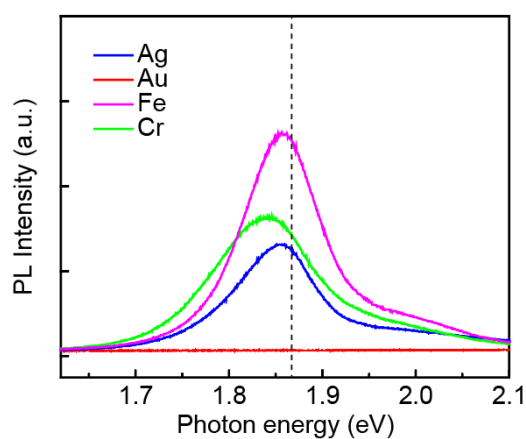


Figure S11. PL spectra of the UHV-exfoliated monolayer MoS₂ on Au, Ag, Fe, and Cr films.

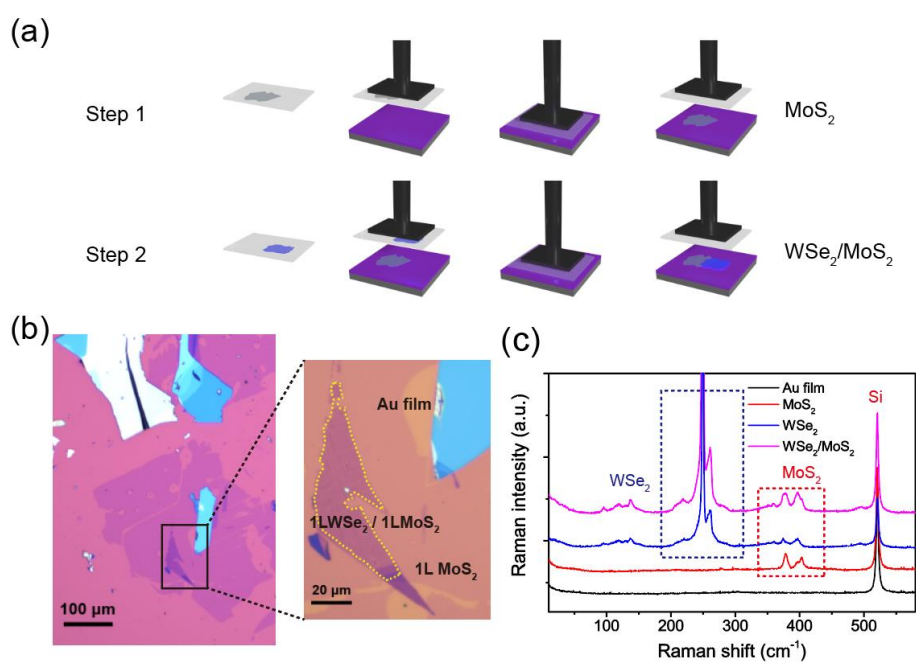


Figure S12. Fabrication of WSe₂/MoS₂ heterostructures in UHV. (a) Schematic diagram of the stacking process. (b) Optical images of the WSe₂/MoS₂ sample. The heterostructure consists of 1L WSe₂ on 1L MoS₂. (c) Raman spectra acquired on the Au film, 1L MoS₂, 1L WSe₂, and the heterostructure, respectively.

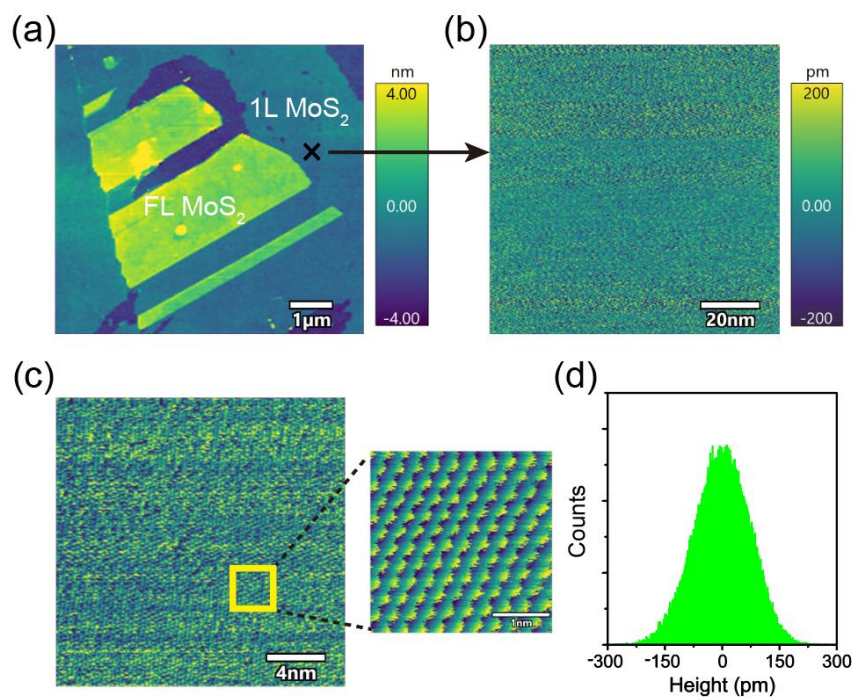


Figure S13. (a-c) AFM images of the UHV exfoliated MoS₂/SrTiO₃(100). The magnified view in (c) shows the atomic resolution. (d) Height distribution of (b).

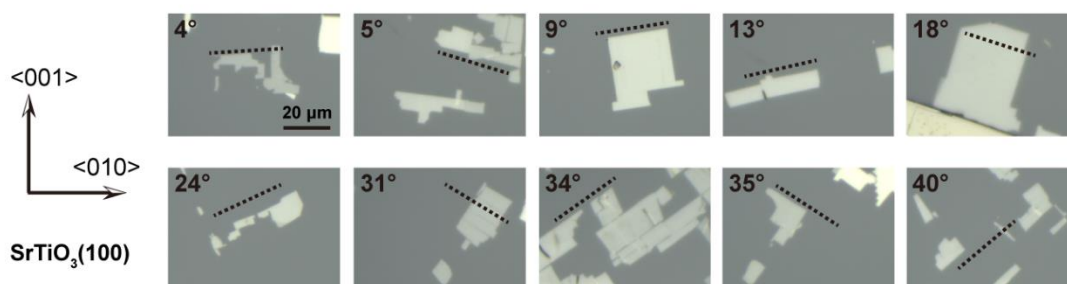


Figure S14. Preparation of ultrathin FeSe on SrTiO₃(100) with different twist angles by UHV exfoliation.

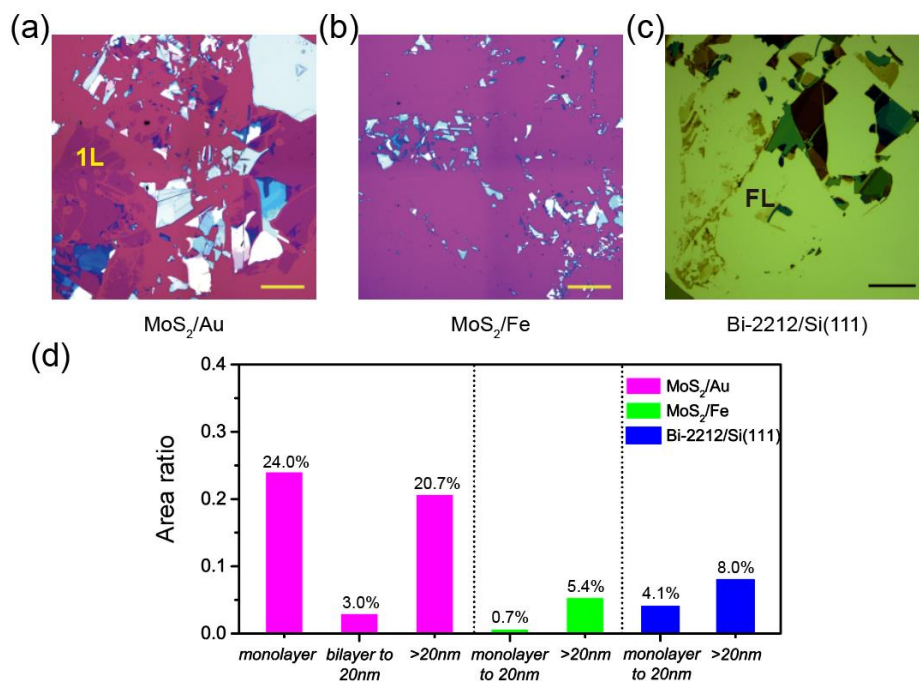


Figure S15. (a-c) Large-scale optical microscope images of the UHV-exfoliated MoS₂/Au, MoS₂/Fe, and Bi-2212/Si(111), respectively. Scale bar: 200 μ m. (d) Area ratios of thin flakes with respect to the substrate with different thicknesses.